

Electrical Conductivity and Polarization Processes in Nanocomposites Based on Isotactic Polypropylene and Modified Synthetic Clay

ANTONIO MOTORI,¹ GIAN CARLO MONTANARI,² ANDREA SACCANI,¹ FRANCESCA PATUELLI¹

¹Dipartimento di Chimica Applicata e Scienza dei Materiali, University of Bologna, Viale Risorgimento 2, 40136 Bologna, Italy

²Dipartimento di Ingegneria Elettrica, University of Bologna, Viale Risorgimento 2, 40136 Bologna, Italy

Received 26 January 2006; revised 26 October 2006; accepted 27 November 2006

DOI: 10.1002/polb.21091

Published online in Wiley InterScience (www.interscience.wiley.com).

ABSTRACT: The direct-current and alternating-current electrical behavior of nanocomposites, formed by isotactic polypropylene partially modified with maleic anhydride and filled with different amounts of modified synthetic clay, has been studied; moreover, the conduction mechanisms and the relaxation processes that take place in the materials have been investigated. The nanocomposites containing small clay contents exhibit direct-current insulating properties comparable to or even higher than those observed in the polymeric matrix. However, as the synthetic clay content increases, the ionic contribution to conductivity becomes considerable. The nanocomposites also show a slightly higher permittivity and loss factor than the host material because of the appearance of a thermally activated relaxation process in the frequency range of 10^{-2} to 10^2 Hz at the investigated temperatures. ©2007 Wiley Periodicals, Inc. *J Polym Sci Part B: Polym Phys* 45: 705–713, 2007

Keywords: dielectric properties; electrically insulating materials; nanocomposites; poly(propylene) (PP); relaxation

INTRODUCTION

Nanocomposites have been the new frontier in materials science since the beginning of the 1990s:^{1,2} the most promising properties of these new materials range from increased thermal resistance, dimensional stability, and flame resistance to higher mechanical properties. More recently, attention has also been focused on their electrical properties: nanocomposites with in-

creased ionic^{3–6} or electronic^{7,8} conductivity, as well as electrorheological properties,⁹ have been produced. However, few results are available on the alternating-current (ac) characteristics,¹⁰ electrical strength,¹¹ and insulating properties of these materials. Some authors have recently investigated the space charge trapping and electrical strength of polymeric nanocomposites for electrical insulation.¹² In this article, the direct-current (dc) electrical conductivity and the ac dielectric permittivity and losses of some nanocomposites, based on partially modified polypropylene and different amounts of modified synthetic clay, are investigated; an insight into the mechanisms of conduction and the relaxation processes is obtained.

Correspondence to: A. Motori (E-mail: antonio.motori@mail.ing.unibo.it)

Journal of Polymer Science: Part B: Polymer Physics, Vol. 45, 705–713 (2007)
©2007 Wiley Periodicals, Inc.

EXPERIMENTAL

Materials

Isotactic polypropylene (iPP) with a weight-average molecular weight of 350,000 g/mol and a melt flow index of 3.2 g (Borealis) was used.

Polypropylene with a number-average molecular weight of 1000 g/mol and with 3.5 wt % maleic anhydride grafted to the backbone of the polymer chains (Clariant) was used. This modification was necessary to increase the polarity of the organic matrix and favor the interaction with the inorganic particles.

Synthetic fluorohectorite (SM; MK 100, CO-OP Chemical Co.) with an average particle size of 1–5 μm and a specific surface area of 9 m^2/g was used. The distance between the different planes of the original clay was 0.95 nm. A synthetic clay was chosen to introduce an amount of impurities as low as possible into the material. The clay was functionalized with octadecylamine (ODA) by an ion-exchange treatment; a further compatibilizer, butyl amine (BA), was also investigated.

The compounding of the thermoplastic nanocomposite materials was performed at 200–230 $^{\circ}\text{C}$ with a Collin ZK 25T corotational twin-screw extruder with a screw speed of 120 rpm and a mass flow of 2 kg/h. The extruder was equipped with a flat film extrusion die, followed by a chill roll unit, which allowed the obtainment of 1-mm-thick films. The compounded materials were thus characterized by a matrix, which was a 80/20 wt % blend of pure iPP and iPP modified with maleic anhydride (this blend is called iPPco) containing different amounts of modified synthetic clay (from 0 to 6 wt %; see Table 1). Moreover, 0.25 wt % of a stabilizer mixture (Irganox 1010 and Irgafos 168) was added.

Table 1. Compositions and Thermal Characteristics of the Investigated Materials

Material	Modified iPP (wt %)	Synthetic Clay (wt %)	T_m ($^{\circ}\text{C}$)	X_c (%)
iPP	0	0	164	30
iPPco	20	0	161	33
IPPco2%	20	2	164	29
IPPco4%	20	4	164	28
iPPco6%	20	6	163	27

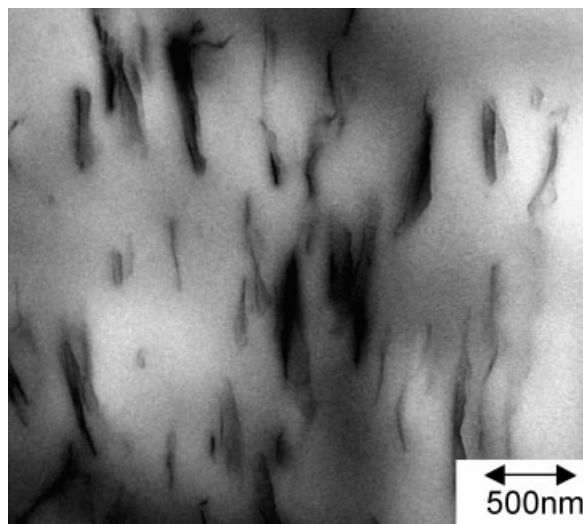


Figure 1. TEM image of the 6% ODA modified nanocomposite.

Measurements

The samples were submitted to dc electrical volt-ampereometric characterization, in the temperature range from 70 to 125 $^{\circ}\text{C}$, according to ASTM Standard D 257 by the application of an electrical field of 1 kV/cm by means of a Keithley 237 voltage generator; dc charging (therefrom conductivity) and discharging currents were recorded up to 7200 s with a Keithley 6514 electrometer. The ac measurements were carried out in the same temperature range from 10^5 to 10^{-2} Hz by means of an Alpha high-resolution dielectric analyzer (Novocontrol).

The formation of a nanocomposite structure in the material containing the ODA-modified synthetic clay was demonstrated by transmission electron microscopy (TEM) observations, as shown in Figure 1.^{13,14}

All materials were subjected to differential scanning calorimetry (DSC; Q10 TA Instruments), to determine the glass transition temperature (T_g), melting temperature (T_m), and degree of crystallinity (X_c) of the polymer matrix; the glass transition was also investigated by dynamic mechanical analysis (three-point-bending geometry, scanning rate = 4 $^{\circ}\text{C}/\text{min}$; DMA 7, PerkinElmer).

RESULTS

Figure 1 shows the structure of the 6% ODA modified material: the exfoliated silicate platelets, which are partially aligned in a preferred

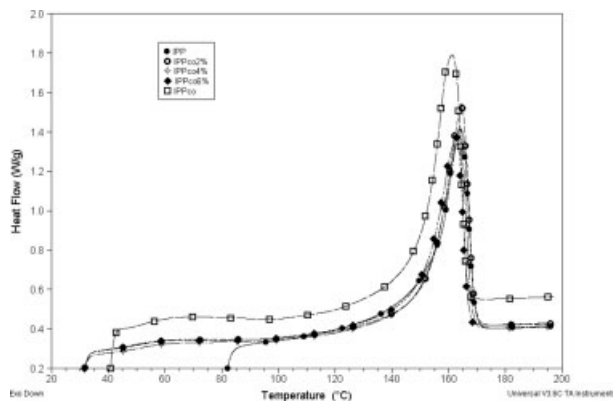


Figure 2. DSC thermograms of the investigated materials.

direction, can be observed. Figure 2 shows the DSC thermograms of all the investigated materials, which are relevant to the melting of the crystalline phase. The thermograms appear to be very similar, both in shape and in the temperature location of the melting peaks. Table 1 reports the T_m and X_c values of the samples. We calculated the crystalline fraction, assuming for all materials a melting enthalpy of 5.8 kJ/mol,¹⁵ which indeed is the value for the crystalline homopolymer; thus, a small error may affect the X_c values because we assumed for iPPco the heat of fusion of the homopolymer and ignored possible effects of SM addition in the nanocomposites. Nevertheless, in agreement with other studies,¹⁶ the overall X_c value remains almost unchanged, although a small decrease can be observed as the SM content increases. As for the T_m values, they increase with a 2% concentration of SM and subsequently decrease until 6% is reached, but the differences are small, confirming that the thickness of the crystalline lamellae in the nanocom-

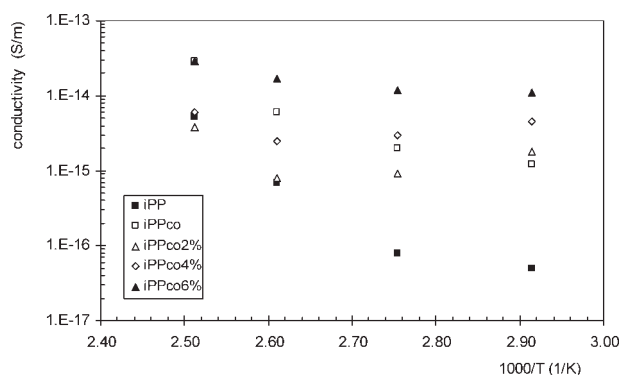


Figure 3. Electrical conductivity versus $1000/T$ at 60 s from the voltage application.

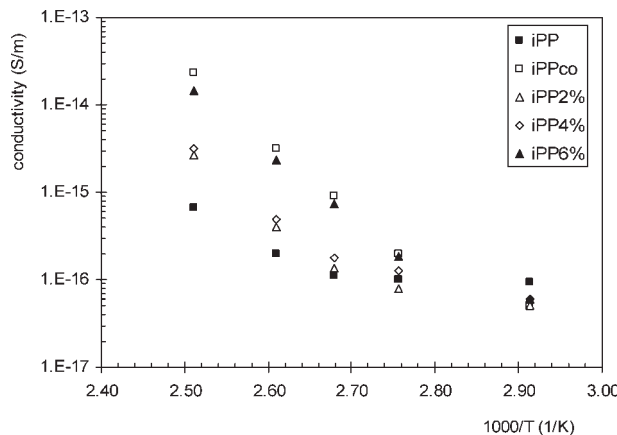


Figure 4. Electrical conductivity versus $1000/T$ at 7200 s from the voltage application.

posites is almost unchanged.^{16,17} Low-temperature thermograms (not reported here) did not allow a clear determination of T_g ; however, measurements carried out by dynamic mechanical analysis disclosed a small dependence of the T_g value on the SM content ($T_g = 14$ °C for iPP, $T_g = 10$ °C for iPPco6%). The dc electrical conductivity of the materials versus the reciprocal of the absolute temperature, over the temperature range of 70–125 °C, is shown in Figures 3 and 4, in which values at 60 (i.e., under transient conditions) and 7200 s (i.e., under quasi-steady-state conditions) after the voltage application are reported. The transient conductivity values of the nanocomposite materials are higher than those of iPP, mainly below 100 °C. On the contrary, under quasi-steady-state conditions, the differences decrease with decreasing temperature, and all samples tend to exhibit similar values at the lowest temperature investigated (70 °C). The activation energy values of the conduction process, calculated from a linear interpolation of

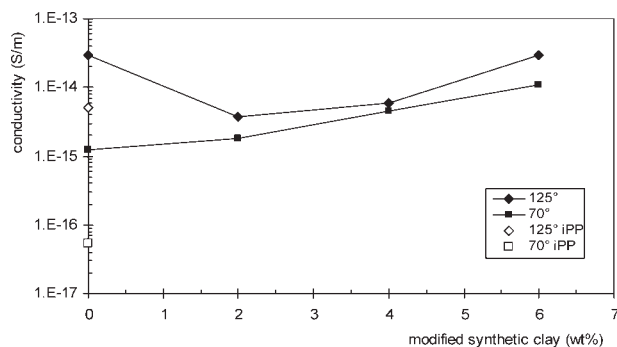


Figure 5. Electrical conductivity versus the modified clay content at 70 and 125 °C after 60 s from the voltage application.

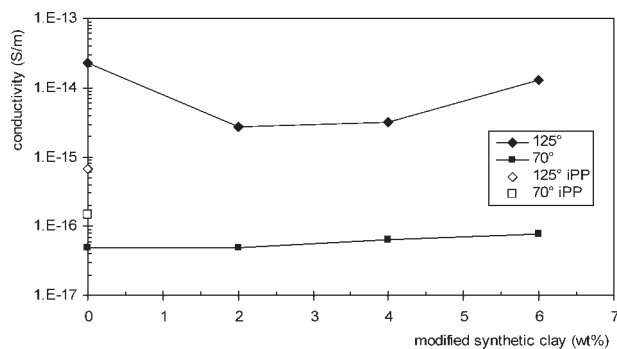


Figure 6. Electrical conductivity versus the modified clay content at 70 and 125 °C after 7200 s from the voltage application.

the data of Figure 4 above 90 °C, are 100 kJ/mol for iPP ($R = 0.929$), 150 kJ/mol for iPPco ($R = 0.943$), and 145 kJ/mol for the nanocomposites ($R > 0.944$). The conductivity at 125 and 70 °C after 60 s of the voltage application is reported in Figure 5 as a function of the SM content. iPPco shows higher conductivity than pure iPP. Moreover, at 125 °C, SM addition causes a conductivity decrease at a low concentration (2 wt %) and then a continuous increase. At 70 °C, an almost linear increase with the clay content can be observed. The plot of the conductivity at the same temperatures and after a charging time of 7200 s is reported in Figure 6. The behavior is qualitatively similar to that of Figure 5, but at 70 °C, all the nanocomposites exhibit conductivity values significantly lower than that shown by pure iPP.

As for the ac properties, Figures 7–10 show the dielectric permittivity and loss factor of iPP and iPPco as functions of frequency and at different temperatures. The pure polymer exhibits the

lowest values of the permittivity (Fig. 7) and loss factor (Fig. 8), whereas for iPPco, the property values tend to increase, mainly below 10 Hz and above 90 °C (Figs. 9 and 10). In Figures 11 and 12, the permittivity and loss factor of iPPco6% are reported versus the frequency at different temperatures (iPPco2% and iPPco4% provided similar plots, which are not reported for the sake of brevity). In all the nanocomposites, a thermally activated relaxation process takes place in the frequency range of 10^{-2} to 10^2 Hz, which produces an absorption maximum in the loss factor curves and a flex in the permittivity curves. The loss factor peak at 125 °C is shown in Figure 13 for the three nanocomposites investigated: an increase in the relaxation intensity with the SM content can be observed. In Figure 14, the frequency of the loss maxima is plotted versus the reciprocal of the absolute temperature for all investigated nanocomposites; an activation energy value of 150 kJ/mol ($R > 0.993$) was calculated from the linear regression of the data for all the nanocomposites. The ac measurements were also carried out on a nanocomposite, based on the iPPco matrix and containing 6 wt % SM modified with BA, to verify the effect of a different clay modifier on the electrical behavior; in Figure 15, loss factor curves as a function of frequency at different temperatures are shown. The relaxation process is still present, but its intensity is lower than that observed in the nanocomposite containing SM modified by ODA, and the loss factor maxima are located at higher frequencies, as can be clearly observed in Figure 14; the activation energy of the process is 80 kJ/mol ($R = 0.997$). Fourier transform of discharging currents (not shown for the sake of brevity) did not

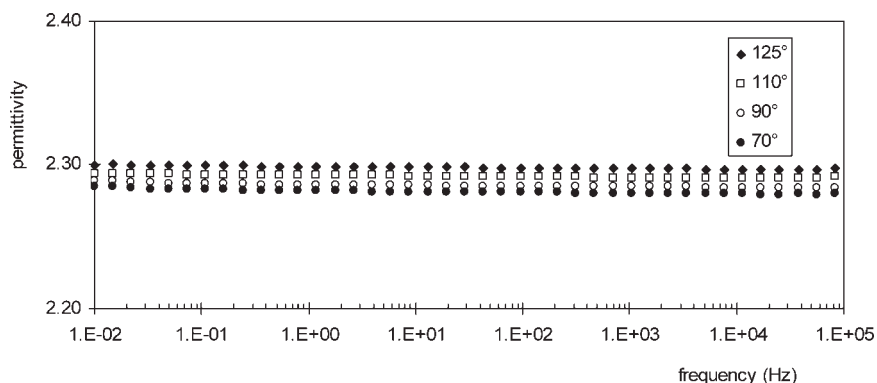


Figure 7. Dielectric permittivity of iPP as a function of frequency at different temperatures.

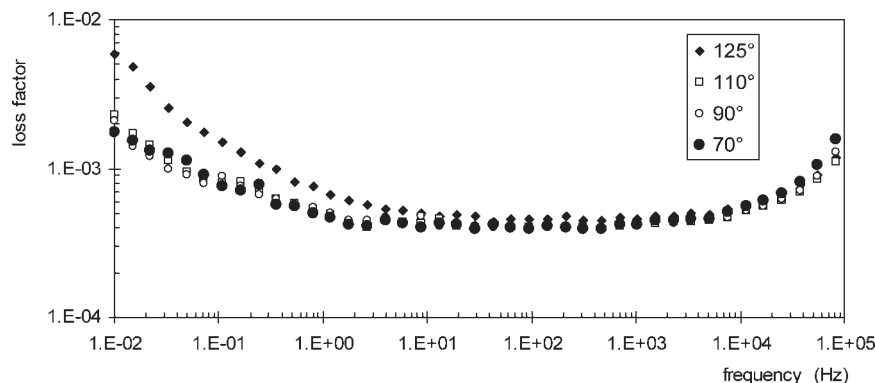


Figure 8. Dielectric loss factor of iPP as a function of frequency at different temperatures.

disclose any further relaxation process in the ultralow frequency range (10^{-2} to 10^{-5} Hz).

DISCUSSION

Concerning the dc behavior of the investigated materials, the presence of the inorganic phase produces two different effects on quasi-steady-state conductivity. At relatively low temperatures (70–90 °C), at which the contribution of the electronic mechanism to conduction prevails,¹⁸ the conductivity slightly increases as the amount of SM increases. Indeed, at 70 °C and 7200 s, the nanocomposite exhibits a lower conductivity. This effect could be ascribed not to the inorganic phase (a negligible effect of the phase content is observed) but to a reduction of mobility and/or concentration of the electronic charge carriers caused by the modification of pure iPP.

At higher temperatures (>90 °C), at which the contribution of the ionic charge carriers largely prevails, the conductivity decreases up to 2 wt %

SM, and then it increases with SM increasing (however, at 6 wt %, it is still a bit lower than that of iPPco). Some considerations must be made to explain the behavior at high temperatures: (1) it can be hypothesized that a limited number of impurities were unavoidably introduced by the SM, either as sodium ions arising from its not complete functionalization or as protons provided by the amine dissociation; (2) the same overall amount of the crystalline phase for all materials was derived from the melting peaks of DSC thermograms; and (3) it can be speculated that nanocomposites have lower permeabilities/diffusivities than the corresponding polymeric matrix because of the longer diffusing pathways inside the structures.^{19,20} Ions diffuse in the amorphous phase of the materials, and because this fraction remains quantitatively unchanged in volume, possible effects of the crystalline phase should be ruled out. Thus, at a low SM content, the prevailing effect should be an increase in the tortuosity of the conducting pathways, which causes a mobility decrease of the ionic charge carriers. Further SM

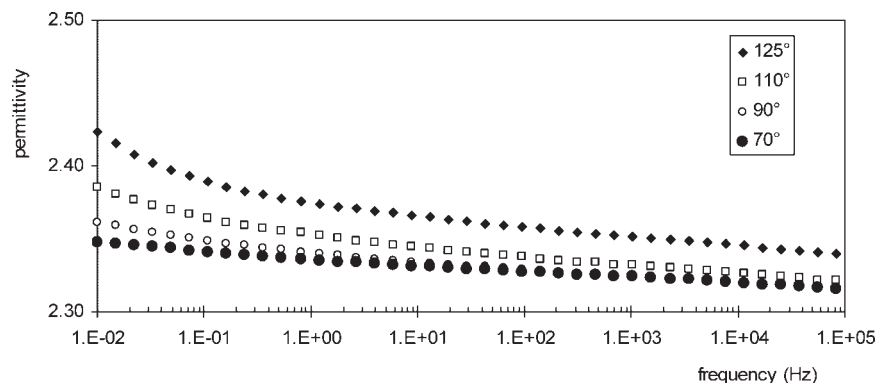


Figure 9. Dielectric permittivity of iPPco as a function of frequency at different temperatures.

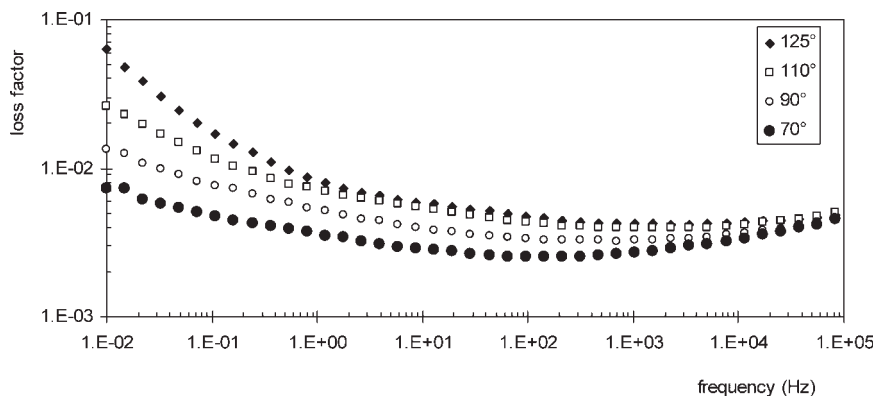


Figure 10. Dielectric loss factor of iPPco as a function of frequency at different temperatures.

addition enhances the ion content up to a quantity that overcomes the tortuosity effect. This is also supported by the observation that some authors have found a reduced distance between the individual silicate layers and thus a lower intercalation of the macromolecular chains with an increasing amount of SM.¹⁶ Therefore, a higher silicate content may not increase the interacting surface between the charge carriers and filler and thus the length of the conducting pathways.

As for the ac behavior, in the power frequency range, the nanostructured materials show higher losses than iPPco above 70 °C because of the presence of the thermally activated dielectric relaxation process previously described, although such an increase does not compromise the use of these materials for high-voltage insulation. First, a dipolar origin of the relaxation process can be

excluded, according to the following observations. The data in Figure 14 (i.e., f_{\max} vs $1/T$) can fit well a linear law, and this seems to rule out that the glass transition of the polymer as the origin of the process; moreover, dynamic mechanical analysis results show that the peaks of the T_g relaxation take place in a rather different region of the transition map. A sub-glass-transition dipolar relaxation, which is related to local vibrations of chain fragments, takes place in iPP at higher frequencies than those evidenced here;^{21,22} indeed, a shift of this relaxation to lower frequencies might take place if a chain-stiffening effect of the filler is assumed, but this possibility is ruled out by the previously discussed results of T_g measurements. Moreover, it has been already underlined that the silicate layers seem to enhance the mobility of the macromolecules.²³ A second hypothesis on

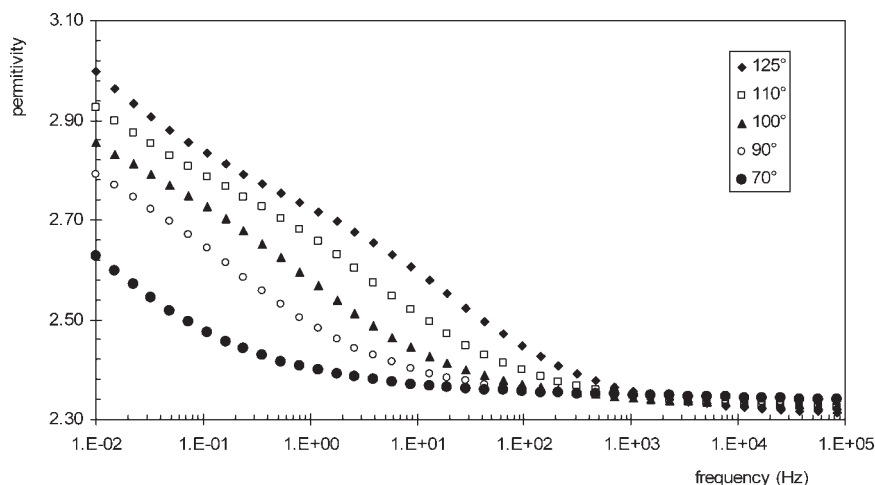


Figure 11. Dielectric permittivity of iPPco6% as a function of frequency at different temperatures.

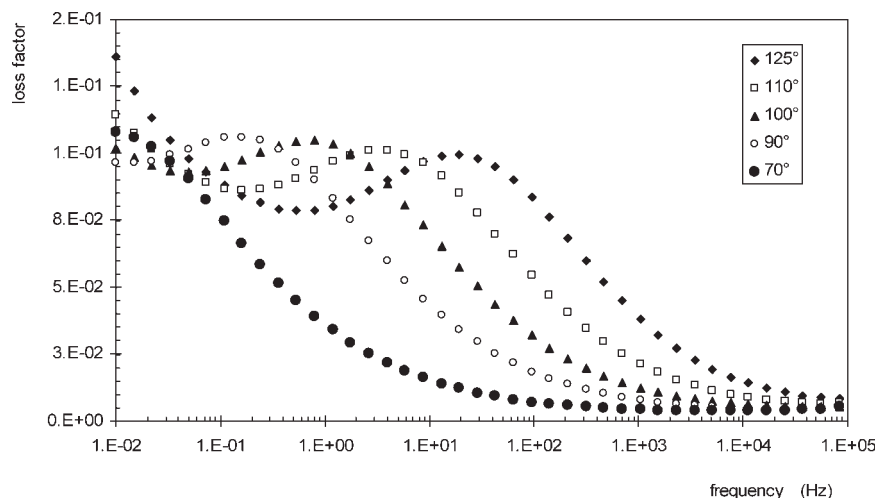


Figure 12. Dielectric loss factor of iPPco6% as a function of frequency at different temperatures.

the origin of the relaxation is related to an interaction between the crystalline phase (mainly the surface of the crystals) and the silicate filler, which could lead to the splitting of the melting peak of the crystalline phase. Again, this is not supported by the results of dynamic mechanical analysis. Therefore, it can be assumed that the relaxation process arises from the charge accumulation at the nanointerfaces [Maxwell–Wagner–Sillars (MWS) type]. This is supported by (1) the closeness of the activation energy values of the conduction and relaxation processes, which points out the same origin of both processes, that is, charge motion, and (2) the increase in the relaxation intensity with increasing SM content and thus in the nanointerface surface. The relax-

ation of the MWS type is usually located at a lower frequency (<10 Hz) than those found for these materials.^{24,25} In this case, it can be speculated that the nanoscale dimension of the interfaces causes a shifting of the relaxation to higher frequencies because of the shorter time required to charge the nanodimensional induced capacitors (i.e., the exfoliated silicate lamellae). Moreover, some authors have found evidence of this type of relaxation in nanocomposites based on polyamide-6.²⁶ Although in this case the material was investigated in the molten state and the permittivity changes were much higher, the origin of this relaxation could be the same. The presence of a relaxation process at higher frequencies and with a lower intensity in the sam-

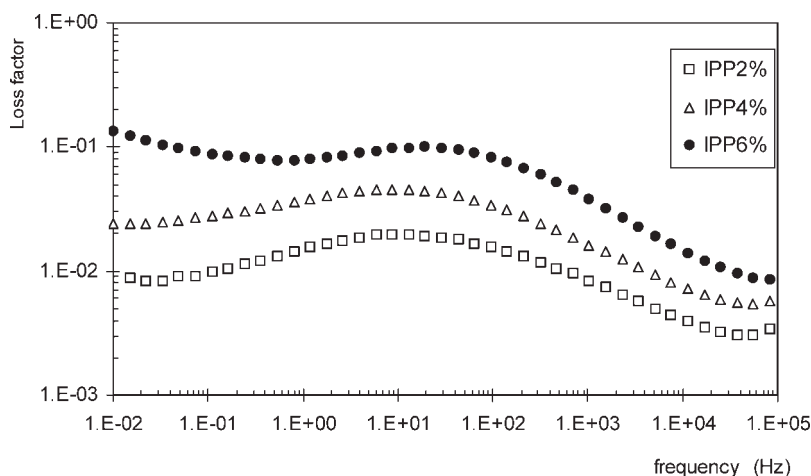


Figure 13. Dielectric loss factor versus the frequency at 125 °C for nanocomposites with different contents of modified clay.

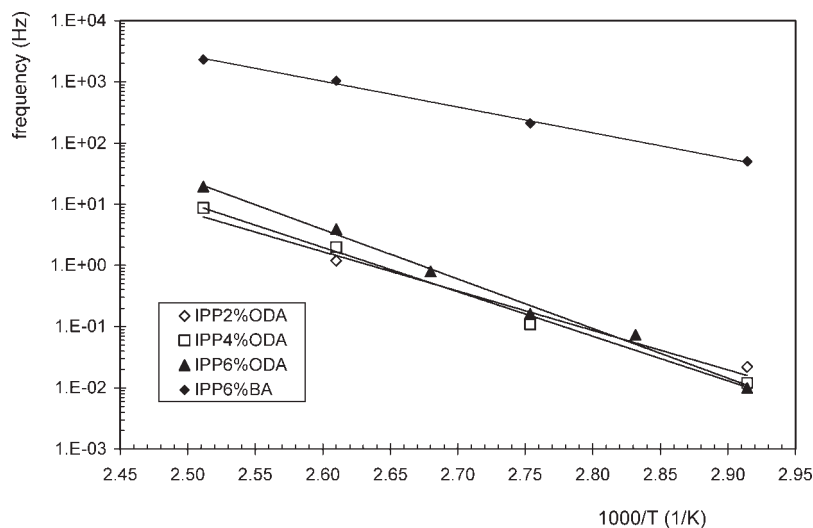


Figure 14. Frequency of the loss factor maxima (f_{\max}) versus $1000/T$ for the investigated nanocomposites.

ple containing BA-modified SM is noteworthy: in previous studies,¹³ on account of the results of mechanical tests, this material was defined as a conventional composite. These results show that probably a partial polymer–silicate interaction is present, leading to a different nanomorphology than that of ODA-modified samples. The extent of this interaction is probably too weak to change the macroscopic mechanical properties of the material, but it is sufficient to affect the dielectric properties. The results discussed here support the usefulness of dielectric spectroscopy for the investigation of the nature and extent of the interactions between the polymer matrix and sil-

icate phase in nanocomposites. Therefore, dielectric spectroscopy can represent an additional tool to the usual techniques, such as TEM, for the investigation of interfaces in nanostructured polymeric materials.

CONCLUSIONS

Nanostructured materials, based on pure and modified iPP filled with a low content of synthetic clay, exhibit good electrical insulating properties, comparable to those of unfilled materials (or even better), because the exfoliated silicate tends to

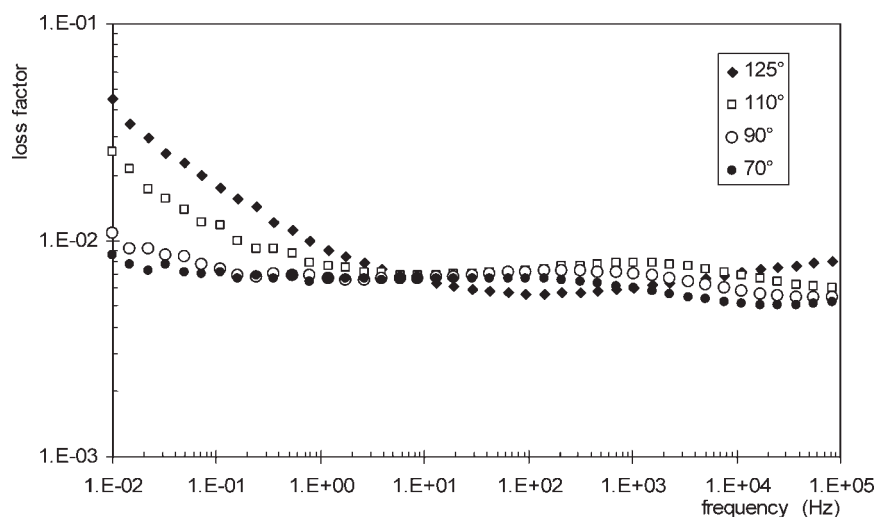


Figure 15. Dielectric loss factor versus the frequency at different temperatures for BA-modified iPPc6% nanocomposites.

reduce the diffusion of ionic charge carriers, thus reducing their mobility mainly at high temperatures. A high silicate content, however, causes a slight decrease in the insulating properties of the nanocomposite.

The presence of the silicate nanophase generates a thermally activated dielectric relaxation process of the MWS type, which slightly affects both the dielectric permittivity and loss factor values.

REFERENCES AND NOTES

- Alexandre, M.; Dubois, P. *Mater Sci Eng R* 2000, 28, 1.
- Suprakas, S. R.; Masami, O. *Prog Polym Sci* 2003, 28, 1539.
- Hwang, J. J.; Liu, H. J. *Macromolecules* 2002, 35, 7314.
- Fan, L.; Dang, Z.; Wei, G.; Nan, C.; Li, M. *Mater Sci Eng B* 2003, 99, 340.
- Chen, H. W.; Lin, T. P.; Chang, F. C. *Polymer* 2002, 43, 5281.
- Chen, W.; Xu, Q.; Yuan, R. Z. *Compos Sci Technol* 2001, 61, 935.
- Yeh, J. M.; Chin, C.; Chang, S. *J Appl Polym Sci* 2003, 88, 3264.
- Zheng, W. G.; Wong, S. C.; Sue, H. J. *Polymer* 2002, 43, 6767.
- Lu, J.; Zhao, X. P. *J Mater Res* 2002, 17, 1513.
- Xiao, M.; Sun, L.; Liu, J.; Gong, K. *Polymer* 2002, 43, 2245.
- Hong, J. I.; Schandler, L. S.; Siegel, R. Martensson, E. *Appl Phys Lett* 2003, 82, 1956.
- Montanari, G. C.; Fabiani, D.; Calmieri, F.; Kaempfer, D.; Thomann, R.; Mulhaupt, R. *IEEE Trans Dielectr Electr Insul* 2004, 11, 754.
- Reichert, P.; Nitz, H.; Klinke, S.; Brandsh, R.; Thomann, R.; Mulhaupt, R. *Macromol Mater Eng* 2000, 275, 8.
- Motori, A.; Patuelli, F.; Saccani, A.; Montanari, G. C.; Mulhaupt, R. *IEEE Annu Rep Conf Electr Insul Dielectr Phenom* 2005, 23, 195.
- Androsch, R.; Wunderlich, B. *Macromolecules* 2001, 34, 8384.
- Nam, P.; Maiti, P.; Okamoto, M.; Kotada, T.; Hasewaga, N.; Usiki, A. *Polymer* 2001, 42, 9633.
- Privalko, V. P.; Dinzhos, R. V.; Privalko, E. G. *Thermochim Acta* 2005, 428, 31.
- Lee, S. H.; Park, J. K.; Hang, J. H.; Suh, K. S. *IEEE Trans Dielectr Electr Insul* 1995, 2, 1132.
- Gorrasi, G.; Tortora, M.; Vittoria, V.; Kaempfer, D.; Mulhaupt, R. *Polymer* 2003, 44, 3679.
- Messersmith, P. B.; Giannelis, E. P. *J Polym Sci Part A: Polym Chem* 1995, 33, 1047.
- Read, B. E. *Polymer* 1989, 30, 1439.
- Wortmann, F. J.; Schulz, K. V. *Polymer* 1996, 37, 819.
- Schmidt, D.; Sha, D.; Giannelis, E. P. *Curr Opin Solid State Mater Sci* 2002, 6, 205.
- Motori, A.; Montanari, G. C.; Gubanski, S. *J Appl Polym Sci* 1996, 59, 1715.
- Nuriel, H.; Kozlovich, N.; Feldman, Y.; Marom, G. *Compos A* 2000, 31, 69.
- Davids, R. D.; Bur, A. J.; McBrearty, M.; Lee, Y.; Gilman, J. W.; Start, P. R. *Polymer* 2004, 45, 6487.